Enhanced dielectrophoresis of nanocolloids by dimer formation

Emppu Salonen,[1] Emma Terama,[1] Ilpo Vattulainen,[2,1,3] and Mikko Karttunen[4]

[1] *Laboratory of Physics and Helsinki Institute of Physics, Helsinki University of Technology, Finland* *
[2] *Memphys–Center for Biomembrane Physics, Physics Department, University of Southern Denmark, Odense, Denmark*
[3] *Institute of Physics, Tampere University of Technology, Finland* †
[4] *Department of Applied Mathematics, The University of Western Ontario, London, Ontario, Canada* ‡

We investigate the dielectrophoretic motion of charge-neutral, polarizable nanocolloids through molecular dynamics simulations. Comparison to analytical results derived for continuum systems shows that the discrete charge distributions on the nanocolloids have a significant impact on their coupling to the external field. Aggregation of nanocolloids leads to enhanced dielectrophoretic transport, provided that increase in the dipole moment upon aggregation can overcome the related increase in friction. The dimer orientation and the exact structure of the nanocolloid charge distribution are shown to be important in the enhanced transport.

PACS numbers: 82.70.Dd,47.57.jd,82.20.Wt

I. INTRODUCTION

Manipulation of microscopic particles with external electric fields, electrokinetics, has gained considerable attention due to applications in nanotechnology and biomedical research [1, 2, 3, 4]. One of the central methods is dielectrophoresis (DEP), the motion of polarizable particles due to a coupling with a non-uniform electric field [5]. Recent studies have attested the versatility of DEP manipulation with carbon nanotubes [6], DNA [7] and biological micro-organisms [8], as well as the assembly of nanowires [9] and biosensor arrays [10]. The relevance of DEP methods to more complex integrated microscopic analysis and assembly devices [11] is evident.

It has been demonstrated that particles down to a few nm in size can be manipulated with DEP [12, 13], but it is still not known what is the minimum size of particles that can be efficiently transported and trapped [4]. Experiments are hampered by the fact that *in situ* tracking of nanoscale particles is very difficult. With decreasing particle size the effect of thermal noise becomes increasingly important. Furthermore, the motion of polarizable particles in non-uniform electric fields is inherently a non-equilibrium process, and particles in close contact may interact via non-additive many-body interactions. Given these challenges, it is fair to say that understanding the problem of nanoscale DEP calls for new theoretical insight.

For an isolated particle much smaller than the characteristic length of the electric field non-uniformity, the DEP force is given by the well-known expression [2]

$$\vec{F}_{\mathrm{DEP}} = (\vec{p}\cdot\nabla)\vec{E}, \tag{1}$$

where $\vec{p}$ is the particle dipole moment induced by the field $\vec{E}$. As the separation between particles decreases, their mutual interactions lead to modifications in their electric polarizations and the DEP force affecting them [2, 14, 15]. It has been suggested that such changes result in enhanced electrokinetic trapping efficiencies at non-dilute conditions [16]. Controlled particle aggregation may in fact be an efficient way to overcome the large thermal forces that hinder DEP trapping and transport. Despite their importance, these issues, to our knowledge, have not yet been studied neither experimentally nor theoretically in detail. As for non-equilibrium simulations of DEP, there is only one recent study focusing on the transport of an individual nanocolloid [17].

In this letter, we consider DEP through theory and modeling and show how enhanced DEP transport can be obtained by controlled complexation. We use molecular dynamics simulations to study the aggregation and subsequent DEP transport of a dimer comprised of two spherical nanocolloids. We compare the transport properties of a dimer to those of a single nanocolloid, and analyze the competing roles of DEP force and friction.

II. SIMULATION MODEL

Our model [17] is summarized as follows. We start from a charged spherical macroion with N_i small microions, each of charge $q = +2e$, electrostatically bound on the macroion. The macroion charge was set to $Q = -N_i q$, so that the macroion-microion complex, termed hereafter as *nanocolloid*, is charge-neutral. For excluded volume interactions we used a shifted repulsive Lennard-Jones potential, $\Phi_{\mathrm{WCA}} = 4\varepsilon[(\sigma/\{r_{ij}-r_0\})^{12} - (\sigma/\{r_{ij}-r_0\})^6 + 1/4]$, where ε and σ are the characteristic energy and length of the interaction, respectively, and $r_{ij} = |\vec{r}_j - \vec{r}_i|$ is the center-to-center distance between particles i and j. The potential was truncated at $r_{ij} = r_0 + 2^{1/6}\sigma$. The hard-core radius r_0 describing particle size was assigned a non-zero value in interactions involving macroions. Electrostatic interactions were calculated directly from Coulomb's law using a constant relative permittivity ϵ_r, given by $(4\pi\epsilon_0\epsilon_r)^{-1} = 56\,\varepsilon\sigma/e^2$, where ϵ_0 is the vacuum permittivity. These types of generic models are physically transparent and have previously been employed in studies of electrokinetic phenomena in colloidal solutions [18, 19, 20, 21]. Our choice of simulation parameters can be viewed to model, *e.g.*, DEP of reverse micelles [22], reverse phase emulsions

*Electronic address: emppu.salonen@hut.fi
†Electronic address: vattulai@csc.fi
‡Electronic address: mkarttu@uwo.ca

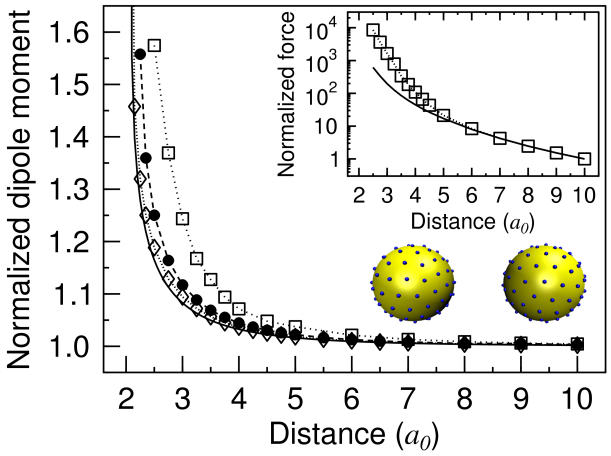

FIG. 1: Dipole moments for two nanocolloids aligned parallel to the electric field, $E_0 = 0.96\,\varepsilon/e\sigma$, normalized with the dipole moment of a single nanocolloid. The symbols correspond to $N_i = 10$ (open squares), 100 (filled circles), and 300 (open diamonds). The solid line is the analytical continuum result [14]. Inset: Total nanocolloid–nanocolloid attractive force for $N_i = 10$ (open squares), normalized with the value at $D = 10\,a_0$. The solid line shows the pure dipole-dipole contribution to the electrostatic force.

[23], or high-generation dendrimers [24].

III. RESULTS AND DISCUSSION

We first studied the influence of nanocolloid interactions on the dipole moments and the resulting electrostatic forces. The calculations were carried out in the absence of solvent. We considered the two specific cases where the line joining a pair of symmetric nanocolloids was either perpendicular or parallel to the direction of a constant electric field $E_0 = 0.96\,\varepsilon/e\sigma$. We used hard-core radii r_0 = 4.5, 16.9, and 29.6$\,\sigma$ for the macroions, with a fixed microion surface density in all cases. The number of microions then increased with r_0 (N_i = 10, 100, and 300, respectively). The macroions were set a distance D apart from each other and subsequently held fixed at these positions. The microions were allowed to move freely, and their surface configurations were relaxed by slowly quenching the kinetic energy from the system with the Berendsen thermostat [25].

Figure 1 shows the nanocolloid dipole moments for a pair aligned parallel to the electric field as a function of the nanocolloid separation D (in units of $a_0 = r_0 + \sigma/2$). The solid line shows the analytical prediction in the continuum limit [14]. For maximal polarization, we chose the value $b = 1$ in eq. (7) of ref. [14]. For the largest macroion ($N_i = 300$) the enhancement in the dipole moments is in excellent agreement with the continuum case. Though, as expected, the agreement becomes worse with decreasing macroion size. This results from the small number of microions and pronounced discrete nature of the microion distribution. Yet it is remarkable how well the continuum theory grasps the essential features even just for $N_i \sim 100$. The results for the case of nanocolloids aligned perpendicular to the electric field also followed the same trend (data not shown): reduction of the dipole moment with decreasing interparticle distance, as follows from eq. (8) in ref. [14], was the most significant for $N_i = 10$. Again, for $N_i = 300$ our simulations were in an excellent agreement with the analytical result.

The inset in fig. 1 shows the electrostatic force between the nanocolloids ($N_i = 10$) as a function of distance, together with just the bare dipole-dipole contribution. As the interparticle distance decreases, the total electrostatic force reaches a value over an order of magnitude larger than the dipole-dipole contribution. By running a series of consecutive kinetic energy quenching simulations at decreasing values of D, an electrostatically bound dimer was formed. Some of the microions were trapped in the region between the macroions. For $E_0 \geq 0.96\,\varepsilon/e\sigma$, the resulting dimer dipole moments were a factor of 3.4 – 4.1 higher than for a single isolated nanocolloid. At $E_0 = 0.68\,\varepsilon/e\sigma$ the ratio of dimer and single nanocolloid dipole moments was only 2.1. The above highlights the special nature of nanosized colloids: the smaller the charge, the stronger is the effect on creating asymmetries as the discrete nature of charge becomes important [21]. Here, as the microions are strongly bound, that leads to non-uniform distribution that enhances the dipole for the pair. Note that a naive estimate, based on the notion that polarization is proportional to volume, would imply only an increase by a factor of two for the nanocolloid dimer. Here, at the higher values of E_0, the increase in the dipole moments is much larger.

To fully describe the dynamics, we next simulated the DEP motion of a dimer with $r_0 = 4.5\,\sigma$ and $N_i = 10$. We chose a spherically symmetric field, $\vec{E}(R) = E_0(R_0/R)^2\vec{e}_{\rm R}$, where R is the radial distance from the electric field interaction center, $R_0 = 1500\,\sigma$ the characteristic length of the field, and $\vec{e}_{\rm R}$ is the radial unit vector. To model DEP transport in a mesoscopic electric field geometry, with proper changes in the electric field strength, we employed an additional electric field system frame of reference and a periodic particle shifting scheme [17]. The initial center-of-mass (CM) position of the dimer was set at $R = R_0$, with the line joining the macroions parallel to the electric field. A detailed description of our simulation protocol is given elsewhere [17].

The dimer was immersed in an explicit solvent of neutral particles with a density of $\rho_s = 0.3\,\sigma^{-3}$. A cubic simulation cell of side length 45$\,\sigma$ was used. Tests with larger systems showed that this cell size resulted in minimal finite-size effects. The solvent density in our coarse-grained model is different from the ones used in simulations of atomic or molecular liquids, where typically $\rho_s \approx 0.8\,\sigma^{-3}$. The solvent density in this letter was also used in the molecular dynamics study of electrophoresis by Tanaka and Grosberg [18], as well as in our previous paper on nanocolloid dielectrophoresis [17]. The motivation for using $\rho_s = 0.3\,\sigma^{-3}$, is that by reducing the solvent friction, related to ρ_s, it is possible to study the effect of the spatial variance of the electric field to the DEP transport with simulations of reasonable length. Second, as we compare the DEP displacements of single nanocolloids and dimers [see below eq. (2)], the solvent density has no major importance to the ratio of the displacements, and thus, to the main conclu-

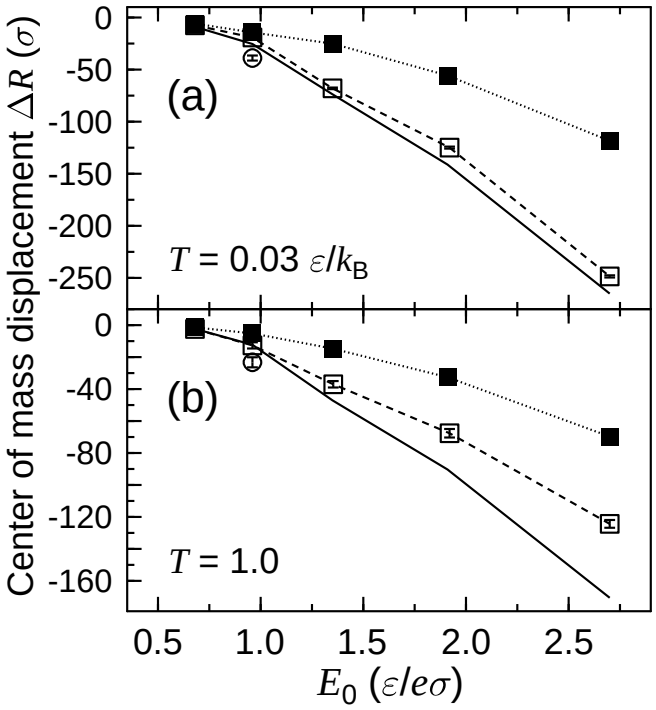

FIG. 2: Mean radial DEP displacements at (a) $T = 0.03$, and (b) $1.0\,\varepsilon/k_{\rm B}$. The open (solid) squares show the data for dimers (single nanocolloids). The open circles at $E_0 = 0.96\,\varepsilon/e\sigma$ show the data only for the simulations where the dimer assumed the higher dipole moment charge configuration (see text) for the whole length of the simulation. The solid lines show the predictions for the dimer case, see eq. (2).

sions of this letter.

For each combination of E_0 and temperature T we carried out 50 – 160 independent DEP simulations of length $5785\,\tau$, with the unit of time given by $\tau = \sigma\sqrt{m/\varepsilon}$. To give a concrete idea of the timescales involved, with the central quantities in our model having plausible nanocolloid values σ = 0.2 nm, m = 30 amu (atomic mass unit), $\varepsilon = k_{\rm B}T_0$, and T_0 = 300 K, our simulations would then correspond to a timescale of $\approx$ 4 ns. No dimer breakups were observed in the simulations.

Figure 2 shows the dimer and single nanocolloid [26] CM mean radial displacements in the electric field system of reference for the two extreme temperatures used, $T = 0.03$ and $1.0\,\varepsilon/k_{\rm B}$. At $E_0 \geq 1.35\,\varepsilon/e\sigma$ the dimer displacements are clearly larger than those of the single nanocolloid. For $E_0 = 0.68\,\varepsilon/e\sigma$ the DEP displacements are the same within the error bars.

For $E_0 = 0.96\,\varepsilon/e\sigma$ it was observed that the dimer polarization relaxed to two different states, corresponding to two different configurations of the microions trapped between the macroions. In some simulations the dimer assumed a state of very strong polarization with a dipole moment a factor of 5 higher than that of a single nanocolloid. The fraction of simulations with this strong dimer polarization increased with T from 15% at the lowest T to 33% at the highest T used. For the other, more common, polarization state the dipole moment ratio was only 2.1, *i.e.*, a value similar as for $E_0 = 0.68\,\varepsilon/e\sigma$. A more detailed analysis showed that in some cases the dipole made transitions between the two states. However, the dimers never retained the original polarized state that was formed in the absence of the solvent. Similar transitions were not observed for any other value of E_0.

Equation (1) shows that the DEP force affecting a dimer is larger than that on a single nanocolloid. But the frictional force due to the solvent on the dimer is also larger. Figure 2 shows that in our case the DEP force acting on the dimer outweighs the increase in friction. Whether the DEP transport of aggregates is enhanced in comparison to single particles *in general* is essentially determined by the relative changes in these two factors. An estimate for the ratio of the friction factors of a dimer and a single spherical nanocolloid, ξ_2/ξ_1, can be made from hydrodynamics of smooth particles. With the long axis of the dimer aligned with the direction of motion, $\xi_2^{\parallel}/\xi_1 \approx 1.29$ [27]. For motion perpendicular to the long axis of the dimer, $\xi_2^{\perp}/\xi_1 \approx 1.43$. This strongly suggests that nanocolloid aggregation enhances DEP transport, in line with our results in fig. 2; see also discussion below.

To elaborate this issue, note that it has previously been verified [17] that DEP displacements with the range of external parameters E_0 and T used here are linearly proportional to the mean DEP force. A simple estimate for the dimer DEP displacement, ΔR_2, is then obtained from,

$$\Delta R_2 \approx \frac{F_2(R_0)}{F_1(R_0)} \left(\frac{\xi_1}{\xi_2^{\parallel}}\right) \Delta R_1, \qquad (2)$$

where $F_i(R_0)$ is the initial DEP force on the system consisting of i nanocolloids at R_0, and ΔR_i its displacement at the corresponding E_0. The resulting values are shown as solid lines in fig. 2. The agreement with the simulation data at $T = 0.03$ $\varepsilon/k_{\rm B}$ is good, though eq. (2) does not properly account for the spatial dependence of the DEP force.

At increasing temperatures it should be expected that the rotational motion of the dimer hinders its DEP transport. This is due to two effects. First, for orientations deviating from full alignment with the direction of motion the effective friction factor of the dimer increases, see above. Second, the dipole moment of the rotating dimer changes as the microion distribution relaxes according to the field. Although changes in the microion surface distributions resulted, on the average, in appreciable DEP forces at all orientations, perpendicular dimer orientation with respect to the direction of $\vec{E}$ decreased the coupling strength up to by a factor of two. Considering the increased friction (by a factor of $\sim$1.43) together with the relaxation of the microion distribution, decreasing the DEP force by 50%, an increase of $\vec{F}_{\rm DEP}$ by a factor of $\sim$3 is required for enhanced DEP transport of the nanocolloid dimer when rotations take place.

Interestingly, the dimer serves as a model to gain insight into the role of T on rotational DEP motion of rod-like molecules. The external field counters the dimer rotation by exerting an electrostatic torque $\vec{\Gamma} = \vec{p}_2(R,\theta) \times \vec{E}(R)$, where the dipole moment of the dimer, $\vec{p}_2$, depends on the radial position R and the orientation angle θ with respect to the electric field. The characteristic time of dimer rotation may be shorter

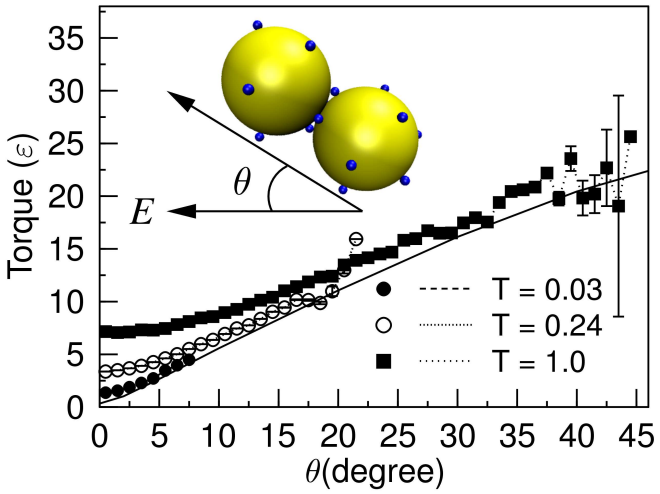

FIG. 3: Electrostatic torque Γ on the dimer as a function of the dimer orientation, E_0 = 1.91 $\varepsilon/e\sigma$. The solid line shows the results calculated for a relaxed charge distribution.

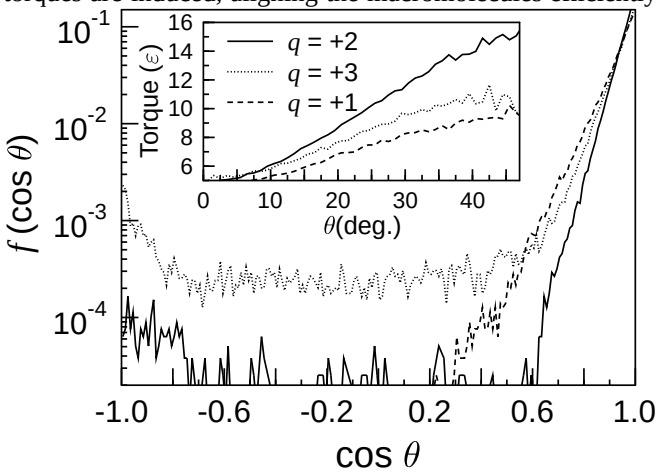

FIG. 4: Distributions of the dimer orientations with respect to $\vec{E}$ in simulations with E_0 = 1.35 $\varepsilon/e\sigma$ and T = 1.0 $\varepsilon/k_{\rm B}$. Inset: values of the electrostatic torque Γ for different microion valences.

than the charge relaxation time. This affects the actual values the dimer dipole moment assumes at different orientations. To illustrate this, we show in fig. 3 the values of torque affecting the dimer. Since the electric field is spatially variant, the data were collected only for $R = 1464-1539\,\sigma$, where $|\vec{E}|$ did not differ by more than 5 % from its value at R_0. We also calculated the torque for fixed dimer orientations in the absence of solvent. The resulting charge distributions then corresponded to the case where the dimer rotation is very slow compared with the microion relaxation time.

For low T the dimer rotations are slow and result in smaller absolute values of Γ. Yet, in comparison to $k_{\rm B}T$, the values of the torque are extremely high and the dimer is efficiently aligned in the direction of the electric field. As T is increased, fluctuations in the microion distributions result in higher values of Γ even for small θ. For lower values of E_0 full rotations of the dimer were also observed.

In addition to the case $q = +2e$ and N_i = 10, we further explored the effects of the microion valence by using two other microion configurations, namely $q = +1e$, N_i = 20 and $q = +3e$, N_i = 7. The orientational distributions of the dimers are shown in fig. 4. Note that the distributions are biased toward $\cos\theta = 1$ due to the initial orientation of the dimer in the simulations. At E_0 = 1.35 $\varepsilon/e\sigma$ and T = 1.0 $\varepsilon/k_{\rm B}$ the DEP displacements for $q = +1e$ and $+3e$ were 19% and 16% smaller, respectively, than for $q = +2e$. These differences were statistically significant with respect to the margins of error. The increased dimer rotation for the two extreme values of valence is also indicated by the smaller values of the electrostatic torque affecting the dimer (cf. inset of fig. 4). These results demonstrate that the microion valence could in fact be a control parameter for nanocolloid DEP motion.

So far rotational effects under DEP have been considered only for much larger objects with large aspect ratios, such as carbon nanotubes [6] and DNA [28]. In these cases large torques are induced, aligning the macromolecules efficiently along the electric field. However, in our case even small perturbations of the microscopic charge distribution due to thermal fluctuations can result in considerable changes in $\Gamma(R,\theta)$, see fig. 3. The rotations could lead to non-negligible hydrodynamic coupling between DEP-manipulated dimers or larger aggregates. Though, as previously mentioned, our modeling can be viewed to correspond to a timescale of a few ns. Since we model a dilute system, possible hydrodynamic effects between rotating dimers are thus not relevant here.

IV. CONCLUSIONS

We have shown how the proximity of nanocolloids with discrete charge distributions increases their DEP coupling. By forming nanocolloid dimers, enhanced transport can be obtained provided that the increase in the dipole moment overcomes the increase in the friction. We have found the rotational motion of dimers to hinder the transport due to smaller DEP coupling and larger friction. The microion valence was shown to affect dimer orientation and transport. Our results indicate that controlled aggregation can be an efficient way of overcoming thermal forces and obtaining high-precision DEP particle manipulation at the nanoscale.

Acknowledgments

We thank K. W. Yu and J. P. Huang for valuable discussions. Support from the Academy of Finland, Emil Aaltonen foundation and NSERC of Canada is acknowledged. We thank the Finnish IT Center (CSC), and the DCSC Center at the University of Southern Denmark for computing time.

[1] Hughes M. P.,Nanotechnology **11**, 2000 124.
[2] Jones T. B., Electromechanics of Particles, Cambridge University Press, Cambridge, 1995.
[3] Hughes M. P., Nanoelectromechanics in Engineering and Biology, CRC Press Boca Raton, USA, 2003.
[4] Burke P. J., Encyclopedia of Nanoscience and Nanotechnology, Nalwa H. S. (Ed.), American Scientific Publishers Stevenson Ranch, CA, 2004.
[5] Pohl H. A., J. Appl. Phys, **22** 1951 869.
[6] Kim J. Han C., Nanotechnology **16** 2005, 2245.
[7] Tuukkanen S., Kuzyk A., Toppari J. J., Hytönen V. P., Ihalainen T., Törmä P., Appl. Phys. Lett. **87** 2005, 1.
[8] Markx G. H., Huang Y., Zhou X., Pethig R., Microbiology **140** 1994, 585.
[9] Hermanson K. D., Lumsdon S. O., Williams J. P., Kaler E. W., Velev O. D., Science **294** 2001, 1082.
[10] Gray D. S., Tan J. L., Voldman J., Chen C. S., Biosens. Bioelectr. **19** 2004, 1765.
[11] Reyes D. R., Iossifidis D., Auroux P., Manz A., Anal. Chem. **74** 2002, 2623.
[12] Bezryadin A., Dekker C., Schmid G., Appl. Phys. Lett. **71** 1997, 1273.
[13] Zheng L., Li S., Brody J. P., Burke P. J., Langmuir **20** 2004, 8612.
[14] Huang J. P., Karttunen M., Yu K. W., Dong L., Phys. Rev. E **67** 2003, 021403.
[15] Huang J. P., Karttunen M., Yu K. W., Dong L., Gu G. Q., Phys. Rev. E **69** 2004, 051402.
[16] Müller T., Gerardino A., Schnelle T., Shirley S. G., Bordoni F., de Gasperis G., Leoni R., Fuhr G., J. Phys. D.: Appl. Phys. **29** 1996, 340.
[17] Salonen E., Terama E., Vattulainen I., Karttunen M., Eur. Phys. J. E **18** 2005, 133.
[18] Tanaka M. Grosberg A. Y., Eur. Phys. J. E **7** 2002, 371.
[19] Linse P. Lobaskin V., Phys. Rev. Lett. **83** 1999, 4208.
[20] Messina R., Holm C., Kremer K., Phys. Rev. Lett. **85** 2000, 872.
[21] Patra M., Patriarca M., Karttunen M., Phys. Rev. E **67** 2003, 031402.
[22] Hakoda M., Nakamura K., Enomoto A., Hoshino T., J. Chem. Eng. Japan **29** 1996, 300.
[23] Flores-Rodriguez N., Bryning Z., Markx G. H., IEE Proc.-Nanobiotechnol. **152** 2005, 137.
[24] Jääskeläinen I., Peltola S., Honkakoski P., Mönkkönen J., Urtti A., Eur. J. Pharm. Sci. **10** 2000, 187.
[25] Berendsen H. J. C., Postma J. P. M., van Gunsteren W. F., DiNola A., Haak J. R., J. Chem. Phys. **81** 1984, 3684.
[26] Single nanocolloid data for $E_0 \geq 0.96\varepsilon/e\sigma$ is from ref. [17]. The data for $E_0 = 0.68\varepsilon/e\sigma$ were simulated in the present study.
[27] Swanson E., Teller D. C., de Haën C., J. Chem. Phys. **68** 1978, 5097.
[28] Germishuizen W. A., Tosch P., Middelberg A. P. J., Wälti C., Davies A. G., Wirtz R., Pepper M., J. Appl. Phys. **97** 2005, 014702.